(6－9)減圧式逆流防止器における弁差圧と流量の関係を利用した異常検知手法の開発に関する研究

○林田　武志(国立保健医療科学院)　伊藤　雅喜(国立保健医療科学院)
門田　卓三(堺市上下水道局)　斉藤　孝志(岡山市水道局)
菊池　良和(佐久水道企業団)

1. 本研究の目的

逆流防止装置の異常検知手法の開発を目的として研究を行い、バネ式の単式逆止弁、二重式逆止弁の各種条件における弁差圧と流量の挙動を基にした検知方法を一昨年度、昨年度に発表している[1) 2)]。本年度の研究対象とした減圧式逆流防止器は、弁異常時には逃がし弁からの排水機能を有し、吐水口空間に次ぐ信頼性のある逆流防止器であり、さらに逃がし弁からの排水検知による弁異常の検知手法も確立されている。しかし、弁異常がない場合においても負圧時には逃がし弁からの排水があること、弁異常による逃がし弁からの排水を伴わない逆流の恐れがあることなど、さらなる検討の余地があり、本研究ではこれらを検証するとともに、これまでの研究において提案した弁差圧と流量による異常検知方法の有効性について検討した。

2. 実験方法

本研究では、図－1 に示す実験装置を用い、供試器具として JWWA 規格の口径 20mm の減圧式逆流防止器を設置し、各種条件下における圧力及び流量を計測した。弁異常状態の再現方法としては、主に径 1mm の針金（ピアノ線）を用い、一次側弁のみ、二次側弁のみ、一次側及び二次側弁の両側弁へ針金を噛ませて、比較を行った。供試器具への圧力条件としては正圧（加圧タンク圧力を 0.2 または 0.4MPa に設定)、逆圧(正圧状態後、二次側増圧、一次側減圧) 及び負圧 (正圧状態後、加圧停止、負圧－54kPa 発生）とした。また、負圧時における実験条件として実使用条件を想定し、供試器具二次側から水槽による 4kPa の逆圧を発生させた。

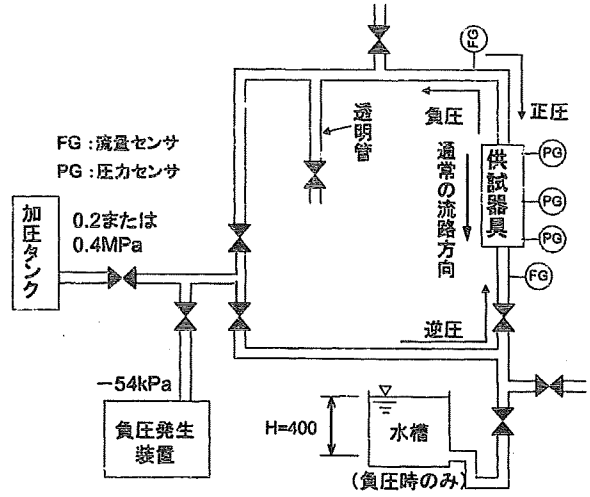

図 - 1　実験装置

3. 実験結果

図－2 に弁正常時（針金なし）及び弁異常時の正圧状態における弁差圧－一次側流量特性の一例を示す。一次側弁異常時、両側弁異常時の場合において常に正の流量が発生している。これは一次側弁異常により逃がし弁から連続的に排水されているためである。また、弁差圧－二次側流量特性では、これまでの他のバネ式逆止弁と同様の傾向を示し、異常時には、正常時の最低作動弁差圧以下で正の流量が発生している。

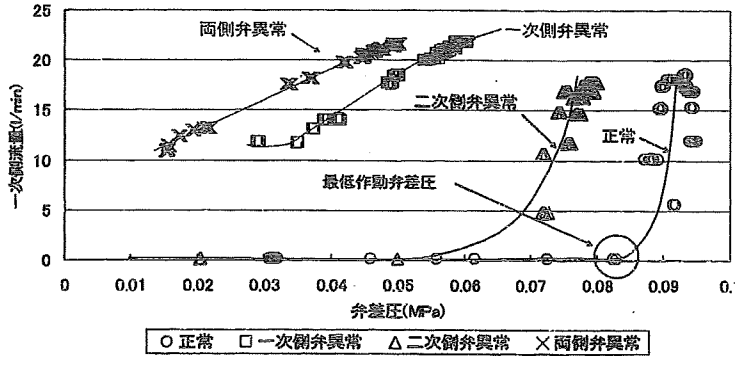

図－2　正圧状態における弁差圧－一次側流量特性の一例（加圧タンク 0.2MPa)

図－3 に逆圧状態における弁差圧－一次側流量特性の一例を示す。両側弁異常時には、一次側流量及び二次側流量の双方で逆流が発生した。特に二次側流量では、より多くの逆流量が発生しており、逃がし弁からの排水機構で大半は排水されるものの少量ではあるが逆流が起こりうることが明

らかとなった。

図－4 に負圧状態における弁差圧－一次側流量特性の一例を示す。両側弁異常時では、一次側流量及び二次側流量の双方において逆流が発生していた。このとき、逃がし弁からの排水は発生しなかった。但し、逃がし弁から空気吸入により、一次側の正確な逆流量が計測できなかったことから、現象を確認するために図―1 の実験装置において供試器具一次側の水抜きを行い、さらに一次側から負圧を発生させ、二次側に設置している水槽の水が透明管に流入するか確認を行った。この結果、やはり逃がし弁からの排水は発生せず、全量が一次側に逆流し、透明管に流入する結果となった。これらのことから、逃がし弁の排水検知による異常検知方法は基本的には有効であるが、まれなケースにおいては、必ずしも十分な手法ではないと考えられる。

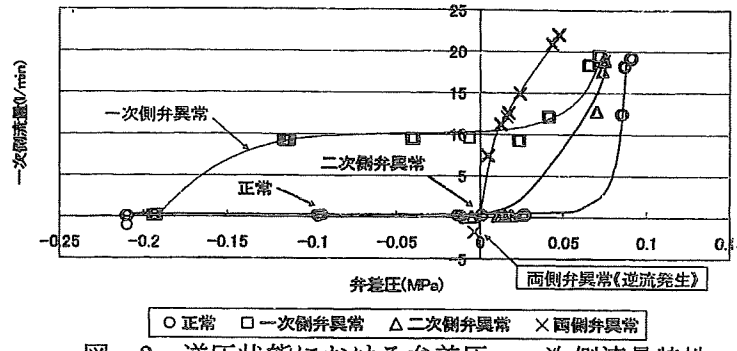

図－3 逆圧状態における弁差圧－一次側流量特性の一例（加圧タンク 0.2MPa）

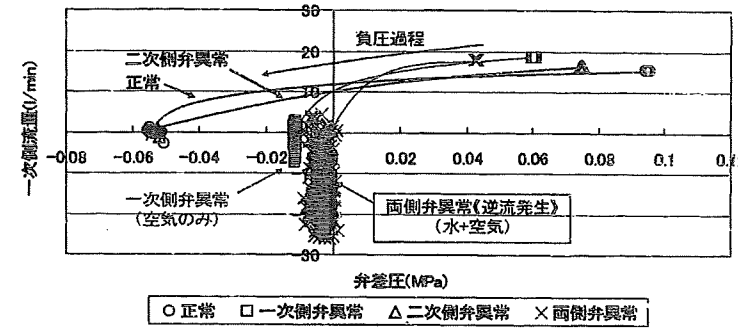

図－4 負圧状態における弁差圧－一次側流量特性の一例（加圧タンク 0.2MPa）

4. 考察

図－5 にこれまでの結果から弁差圧－一次側流量特性を模式化した一次側弁異常時の異常検知条件を示す。正常時の場合、正圧下では最低作動弁差圧以下で流量は 0 であり、それ以後正方向に上昇する。逆圧及び負圧による陰圧下では、それぞれ挙動は微妙に異なるものの最終的に 0 となる。一方、一次側に弁異常がある場合、正圧下では領域 1 に位置し、常に正流量が発生する。陰圧下では、逆圧時と負圧時で挙動が異なり、逆圧時には領域 2 に位置し、負圧時には主に領域 4 に位置する。このように弁差圧－一次側流量特性のいずれの領域に位置しているかを判別することで異常検知が可能である。しかし、どちらかの流量と弁差圧のみでは異常の発生場所の特定までは出来ないので、弁差圧－二次側流量特性においても同様な判定図を作成し、組み合わせて判断することにより、一次側の弁異常、二次側の弁異常等の異常の原因を特定することが可能である。

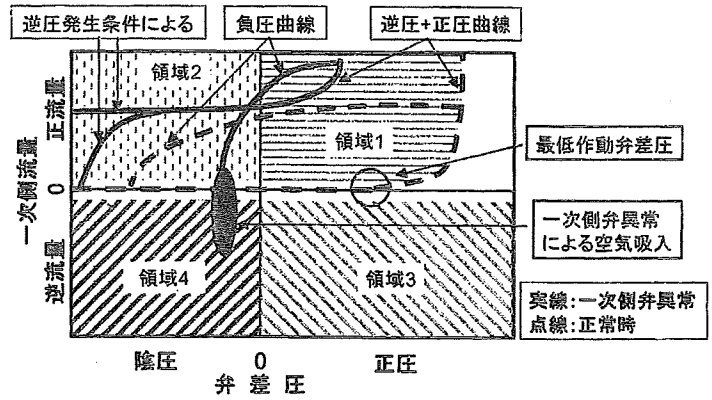

図－5 弁差圧－一次側流量特性による一次側弁異常の異常検知条件

5. まとめ

減圧式逆流防止器は、吐水口空間に次ぐ逆流防止器であるが、最悪の場合には逆流が発生する危険性があり、異常監視システムの構築が必要であること、逃がし弁からの排水検知による異常検知方法も有効ではあるが必ずしも十分とはいえないことが分かった。そのため、これまで提案してきた弁差圧－流量特性を利用した異常検知方法を減圧式逆流防止器に用いることにより、一層の安全性を確保できる給水装置逆流防止システムが構築できると考えられる。

参考文献

1)馬場,伊藤ら:単式バネ式逆止弁の作動状況の可視化と異常検知に関する研究,第 57 回全国水道研究発表会
2)馬場,伊藤:流量・弁差圧の連続監視によるバネ式逆止弁の異常検出手法の開発, 第 58 回全国水道研究発表会

Effects of reversible and irreversible membrane fouling on virus removal by a coagulation–microfiltration system

Nobutaka Shirasaki, Taku Matsushita, Yoshihiko Matsui and Koichi Ohno

ABSTRACT

We evaluated the removal of virus (bacteriophage Qβ) after hydraulic backwashing and the effects of reversible and irreversible membrane fouling on virus removal by a coagulation–microfiltration (MF) system. The rate of virus removal in the coagulation–MF system was low at the beginning of filtration but increased with filtration time, owing to the accumulation of foulant on the membrane. The rate of virus removal thereafter remained high, even after hydraulic backwashing of the membrane to remove reversible membrane foulant. The presence of irreversible, rather than reversible, membrane foulant contributed to the increase in virus removal rate observed at the beginning of filtration. The irreversible membrane fouling maintained a high virus removal rate even after hydraulic backwashing. Moreover, irreversible fouling of the membrane during long-term filtration (1 month) improved virus removal in the coagulation–MF system, and the membrane excluded virus particles even in the absence of coagulation pretreatment. Therefore, the accumulation of irreversible membrane foulant with filtration time played an important role in virus removal by the coagulation–MF system.

Key words | coagulation, membrane fouling, microfiltration (MF), virus removal

Nobutaka Shirasaki (corresponding author)
Taku Matsushita
Yoshihiko Matsui
Koichi Ohno
Division of Built Environment,
Graduate School of Engineering,
Hokkaido University,
N13W8 Sapporo 060-8628,
Japan
Tel.: +81-11-706-7230
Fax: +81-11-706-7279
E-mail: *nobutaka@eng.hokudai.ac.jp*

INTRODUCTION

Microfiltration (MF), which has been extensively applied in the field of drinking water treatment, can effectively remove turbidity, bacteria, algae, and protozoa. However, virus removal is not always possible with MF treatment alone, because MF pore sizes usually are larger than the diameters of pathogenic waterborne viruses. Therefore, pretreatments are required to achieve high virus removal rates.

Coagulation–MF systems remove viruses effectively (Matsui *et al.* 2003; Matsushita *et al.* 2005; Zhu *et al.* 2005*a*,*b*; Fiksdal & Leiknes 2006). However, the rate of virus removal is low at the beginning of filtration and increases with filtration time (Matsushita *et al.* 2005, 2006), suggesting that the accumulation of membrane foulants might contribute to the increase in virus removal rate. In MF without pretreatment, reversible membrane foulant (Jacangelo *et al.* 1995; Madaeni *et al.* 1995), which is removed during hydraulic backwashing, as well as irreversible membrane foulant (Jacangelo *et al.* 1995), which is not removed during hydraulic backwashing, are both reported to contribute to virus removal. However, the characteristics of the membrane foulant differ between systems using MF treatment alone and those combining coagulation and MF. The foulant in MF-only systems would consist mainly of natural organic matter (NOM) and suspended solids (SS) from the source water, whereas that in coagulation–MF systems also would include aluminum floc formed during coagulation pretreatment: the membrane fouling observed in coagulation–MF systems was promoted not only by the NOM and SS themselves but also by the aluminum floc, which contains many types of aluminum species associated with NOM and SS. However, the effects of reversible and irreversible membrane fouling on virus removal in coagulation–MF systems have not previously been investigated.

doi: 10.2166/aqua.2008.048

Accordingly, our objectives were to investigate (1) changes in the virus removal rate after backwashing, and (2) the effects of reversible and irreversible membrane fouling on virus removal in a coagulation–MF system.

MATERIALS AND METHODS

Source water, coagulant, and MF membranes

Water was sampled from the Toyohira River (Sapporo, Japan; Table 1). Polyaluminum chloride (PACl; 10% Al_2O_3, basicity 62.5%; Sumitomo Chemical Co. Ltd., Tokyo, Japan) was used for coagulation pretreatment. The membrane used was a monolithic ceramic MF module (multichannel tubular, nominal pore size 0.1 μm, effective filtration area 0.048 m^2; NGK Insulators, Ltd., Nagoya, Japan), which was installed in a stainless-steel casing.

Virus used

Bacteriophage Qβ (NBRC 20012) obtained from the NITE Biological Resource Center (NBRC, Chiba, Japan) was used as a model virus. The genome of Qβ consists of a single-stranded RNA molecule encapsulated in an icosahedral protein shell (capsid) approximately 0.023 μm in diameter, without an envelope. Qβ is widely used as a surrogate for pathogenic waterborne viruses (Urase *et al.* 1996; Otaki *et al.* 1998) because of its morphologic similarities to hepatitis A viruses and polioviruses, the removal of which is important during the treatment of drinking water. Qβ was propagated for 22 to 24 h at 37°C in *Escherichia coli* (NBRC 13965) obtained from NBRC. The Qβ culture solution was centrifuged (2000 × *g*, 10 min) and then filtered through a membrane filter (hydrophilic cellulose acetate, pore size 0.45 μm; Dismic-25cs, Toyo Roshi Kaisha, Ltd., Tokyo, Japan). The filtrate was purified with a centrifugal filter device (molecular weight cutoff 100,000; Centriplus-100, Millipore Corp., Billerica, MA, USA) to prepare the virus stock solution. Because of this purification, the DOC increase as a result of spiking the river water with the stock solution was reduced to less than 0.1 mg L^{-1}.

Table 1 | River water quality

	River water 1	River water 2
Sampling time	09-Mar-06	12-Dec-06
pH	7.7	7.7
DOC (mg L^{-1})	0.60	1.10
OD260 (cm^{-1})	0.013	0.027
Turbidity (NTU)	0.15	1.13
Alkalinity (mg $CaCO_3$ L^{-1})	19.8	17.6

Virus assay

To measure the concentration of infectious viruses, the PFU method was used in accordance with the agar overlay method (Adams 1959) with the bacterial host *Escherichia coli*. Average plaque counts of triplicate plates prepared from the same sample yielded the virus concentration.

Experimental setup

The experimental setup is shown in Figure 1. The river water in the raw water tank was spiked with virus to a final concentration of $10^{5.8}$ to $10^{7.1}$ PFU $ml^{-1}$and was fed into the system at a constant flow rate (62.5 L(m^2·h)$^{-1}$) by a peristaltic pump. Hydrochloric acid was added before the first in-line static mixer (hydraulic retention time 2.4 s, Noritake Co., Ltd., Nagoya, Japan) to maintain the pH of the MF permeate at 6.8. PACl was injected after the first in-line static mixer and before the second in-line static mixer at a constant dose rate (0, 0.54, 1.08, or 1.62 mg-AlL^{-1}). After the PACl had been mixed in, the water was fed into the ceramic MF module in dead-end mode. Filtration was performed for 0.25, 3, 6, and 12 h with hydraulic backwashing (pressure 500 kPa) with MF permeate or ultrapure

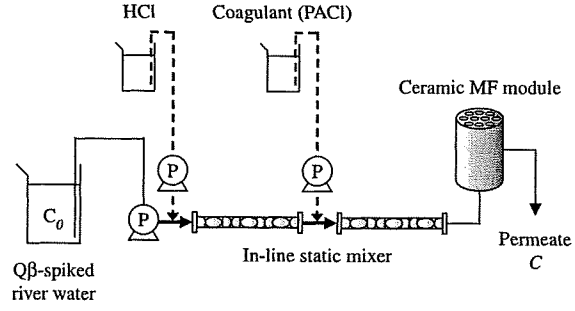

Figure 1 | The experimental coagulation–MF system. C_0 and C are the virus concentrations (PFU ml^{-1}) in the raw water tank and the MF permeate, respectively.

water. Virus concentrations in the raw water tank and MF permeate were measured hourly.

Filtration experiments with the fouled membrane during short-term filtration

Two ceramic MF membranes were fouled with aluminum floc by continuously feeding river water (without spiked virus) into the coagulation–MF system. The PACl dose was 1.62 mg-AlL^{-1} during 6 h of filtration. After 6 h of filtration, one fouled membrane was backwashed with MF permeate (used and backwashed membrane), but the other was not (used membrane without backwashing). Then, during the next 6 h, river water spiked with virus was fed into the system, but no coagulant was injected: virus particles were filtered directly by the membrane. Virus concentrations in the raw water tank and MF permeate were measured hourly.

Filtration experiments with the irreversibly fouled membrane during long-term filtration

The coagulation–MF filtration experiment with hydraulic backwashing was conducted for 1 month at a constant flow rate (62.5 L(m^2·h)$^{-1}$) by using the groundwater at Hokkaido University (DOC 0.48 mgL^{-1}, OD260 0.007 cm^{-1}) without spiked virus. The PACl dose was 1.08 mg-AlL^{-1}, and the backwashing interval was 5 h. After the 1-month filtration, the fouled membrane was backwashed with ultrapure water to remove the reversible membrane foulant (irreversibly fouled membrane). Then, during the next 6 h, river water spiked with virus was fed into the system with or without coagulant. Virus concentrations in the raw water tank and MF permeate were measured hourly.

RESULTS AND DISCUSSION

Effect of hydraulic backwashing on virus removal in the coagulation–MF system

The log of the virus removal rate [log(C_0/C)] in the coagulation–MF system was 4 at the beginning of filtration and gradually increased to 5 over the next 3 h (Figure 2), perhaps because of the presence of reversible or irreversible

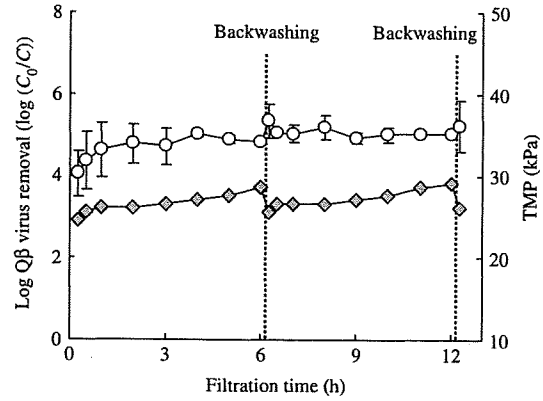

Figure 2 | Changes in the rate of removal of Qβ virus and TMP with filtration time in the coagulation–MF system. Values are the means of 2 experiments. Open circles, rate of Qβ virus removal; solid diamonds, TMP; source water, river water 1; PACl does, 0.54 mg-AlL^{-1}. Backwashing was conducted with MF permeate.

membrane foulant, or both. Our research group previously reported a similar increase with filtration time in the coagulation–MF system (Matsushita *et al.* 2005, 2006). Just after hydraulic backwashing after 6 h of filtration, the transmembrane pressure (TMP) recovered to its initial value (Figure 2). However, the virus removal rate did not decrease to its initial value after backwashing, even though the reversible membrane foulant had been removed, but remained high throughout the subsequent 6 h of filtration. These results suggest that the presence of irreversible membrane foulant would be contributed to virus removal after 6 h of filtration in this coagulation–MF system. The amount of membrane foulant accumulated irreversibly during the 6 h filtration might have been too small to be recognized as an increase in manometric measurement.

To investigate the effects of reversible and irreversible membrane fouling on virus removal during the first 3 h of filtration, when the virus removal rate increased rapidly with filtration time, the membrane was subjected to hydraulic backwashing after 0.25 and 3 h of filtration to remove reversible membrane foulant from the membrane (Figure 3). Although the TMP recovered to its initial value after backwashing at the 3 h time point (Figure 3b), the rate of virus removal did not change significantly (Figure 3a), indicating that irreversible membrane foulant contributed to virus removal. After 0.25 h of filtration, the rate of virus removal increased after backwashing (Figure 3a). Samples

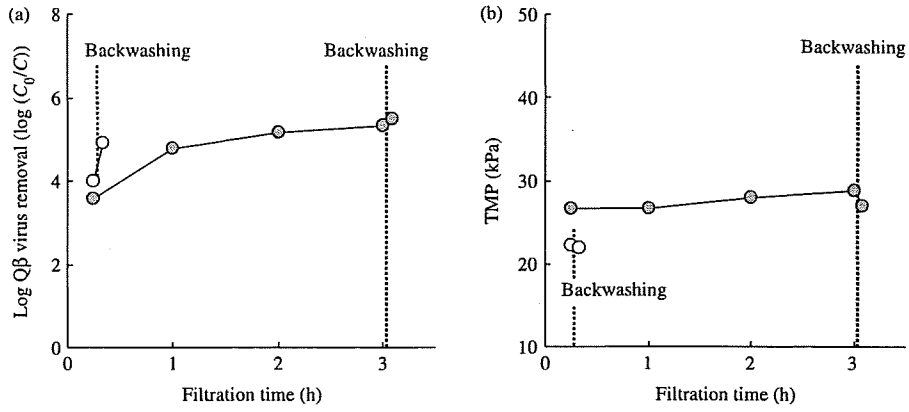

Figure 3 | Effects of reversible and irreversible membrane fouling on Qβ virus removal 0.25 after and 3 h of filtration in the coagulation–MF system. Open circles, 0.25 h of filtration; solid circles, 3 h of filtration; source water, river water 2; PACl does, 1.08 mg-AlL^{-1}. Backwashing was conducted with ultrapure water.

just after backwashing were collected from the system when the filtration was conducted subsequently for 5 min after backwashing. Some foulants might be further accumulated on the membrane during this additional 5 min of filtration; details are not clear. Nonetheless, decrease in virus removal rate was not observed after backwashing at any filtration time (0.25, 3, and 6 h), suggesting that irreversible membrane fouling would contribute to virus removal and that the irreversible accumulation of foulant with filtration time would increase virus removal. In other words, reversible membrane fouling may not affect the virus removal rate in the coagulation–MF system. Our research group reported that the effect of coagulant dose on virus removal in the same coagulation–MF system (Matsushita *et al.* 2005), and suggested that the coagulant dose strongly affected virus removal. However, in this research, the difference in the coagulant dose did not affect the virus removal: although the coagulant doses in Figures 2 and 3 were 0.54 and 1.08 mg-AlL^{-1}, respectively, trends in virus removal were almost the same. These results were possibly due to the difference in source water quality such as DOC, OD260 and turbidity between these two experiments (Table 1). Jacangelo *et al.* (1995) reported that reversible membrane fouling ("cake layer") became the dominant mechanism at early time points during MF filtration without coagulation pretreatment. Our results apparently contradict theirs, probably because of differences in the membrane foulant characteristics in the presence versus absence of coagulation pretreatment.

Characteristics of membrane foulant accumulated during short-term coagulation–MF filtration

To investigate the characteristics of the membrane foulant which accumulated during short-term coagulation–MF filtration, we conducted several filtration experiments. A virgin membrane, devoid of any membrane foulant, could not remove virus particles (Figure 4a). Just after hydraulic backwashing after 6 h of filtration, the TMP of the used and backwashed membrane recovered to its initial value (Figure 4b), and the removal rate of virus particles by the used and backwashed membrane was almost the same as that by the virgin membrane (Figure 4a). Therefore, irreversibly fouled membrane during short-term filtration could exclude the floc with its entrapped virus particles (Figures 2 and 3a) but passed free virus particles (Figure 4a). Although the occurrence of irreversible fouling might reduce the effective pore size of the membrane, the size still might be larger than the diameter of the virus particles.

The used membrane without backwashing, on which membrane foulant accumulated reversibly and irreversibly, achieved a rate of virus removal of 4 log, and it maintained this high rate for 6 h. Therefore, virus particles were rejected by the used membrane without backwashing but not by the used and backwashed membrane (Figure 4a). The difference between the two membranes was the occurrence of reversible membrane fouling; therefore reversible membrane fouling contributed to the removal of virus particles. In contrast, reversible membrane fouling did not contribute to the removal

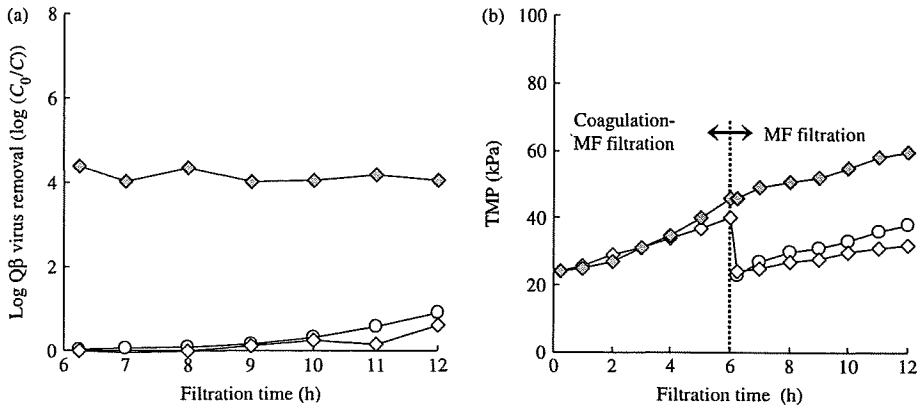

Figure 4 | Characteristics of membrane foulant accumulated during short-term coagulation–MF filtration. Open circles, virgin membrane; open diamonds, used and backwashed membrane; solid diamonds, used membrane without backwashing; source water 1; PACl does, 1.62 mg-AlL^{-1}. The virus was spiked at 6 h of filtration, and MF-only system was operated after that.

of virus particles trapped in floc (Figures 2 and 3a). Perhaps most of the flocs entrapping virus particles were larger than the effective pore size of the used and backwashed membrane: the number of floc particles whose sizes were between the effective pore sizes of the above two membranes was extremely small.

Effects of irreversible membrane fouling during short-term versus long-term filtration

In the above-mentioned experiments, we investigated the effects of membrane foulant which accumulated during short-term filtration (maximum, 6 h). In actual water-treatment plants, membranes are used for prolonged period and undergo repeated backwashing. The membrane gradually is fouled during filtration, such that membrane foulant accumulates irreversibly in the membrane pore structures over time. Figure 5 shows the effect of the irreversible accumulation of membrane foulant on virus removal during long-term coagulation–MF filtration (1 month). The TMP of the irreversibly fouled membrane was much higher than that of virgin membrane at the beginning of filtration (Figure 5b), indicating that membrane foulant accumulated

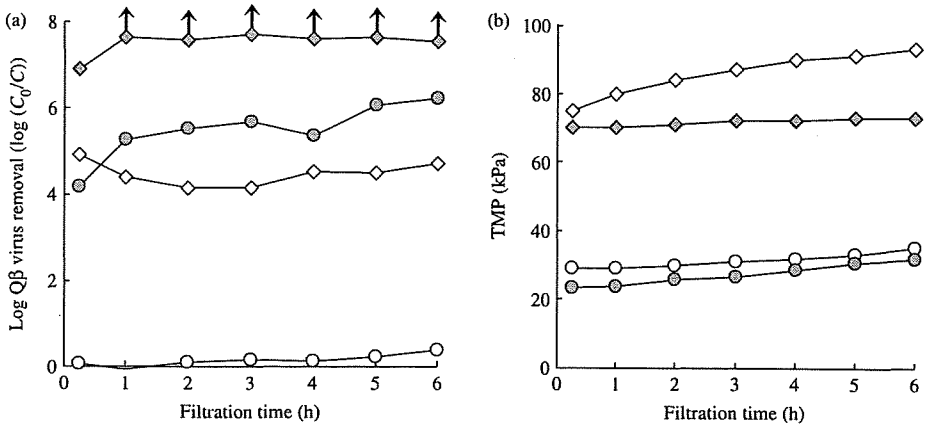

Figure 5 | Characteristics of irreversible membrane foulant accumulated during long-term coagulation–MF filtration. Arrows indicate values greater than those that could be estimated accurately in light of the detection limit of the PFU method. Open circles, virgin membrane in MF-only system; solid circles, virgin membrane in coagulatio–MF system (PACl dose, 1.08 mg-AlL^{-1}); open diamonds, irreversibly fouled membrane in MF-only system; solid diamonds, irreversibly fouled membrane in coagulation–MF system (PACl dose, 1.08 mg-AlL^{-1}); river water 2.

irreversibly and considerably on the membrane in the long-term coagulation–MF filtration experiment.

Whereas the rate of virus removal by a virgin membrane was 5 log in the coagulation–MF system, the rate of virus removal by a membrane that was irreversibly fouled due to long-term filtration was more than 7 log (Figure 5a). These results indicate that the membrane foulant which accumulated irreversibly during long-term filtration improved the virus removal rate in the coagulation–MF system. Although membrane that was irreversibly fouled during short-term filtration could not exclude virus particles (Figure 4a), membrane that was irreversibly fouled during long-term filtration could do so, suggesting that the amount of membrane foulant which accumulated irreversibly during short-term filtration was so small that its effect on the removal of virus particles could not be appreciated. In contrast, when filtration lasted for at least 1 month, the effect was much greater and could be discerned. Jacangelo *et al.* (1995) reported that irreversible fouling of a membrane increased the removal of bacteriophage MS2 during long-term MF filtration; our results agreed with theirs. Even though accidents may occur during coagulation pretreatment in actual coagulation–MF systems and lead to insufficient pretreatment, virus removal still can be expected to some extent, owing to the irreversible accumulation of membrane foulant on the membrane.

CONCLUSIONS

1. The virus removal rate in the coagulation–MF system was low at the beginning of filtration but increased with filtration time owing to the accumulation of foulant on the membrane. The virus removal rate did not decrease and remained high even after hydraulic backwashing of the membrane.
2. Irreversible, rather than reversible accumulation of membrane foulant contributed to the increase in virus removal rate observed at the beginning of filtration. The irreversible membrane fouling maintained the high removal rate of virus, even after hydraulic backwashing.
3. Irreversible fouling of the membrane during long-term filtration improved the virus removal rate in the coagulation–MF system. Moreover, irreversibly fouled membrane excluded virus particles even in the absence of coagulation pretreatment.

ACKNOWLEDGEMENTS

We thank NGK Insulators, Ltd. (Nagoya, Japan) for partly funding this research.

REFERENCES

Adams, M. H. 1959 *Bacteriophages*. Interscience, New York, NY, USA.

Fiksdal, L. & Leiknes, T. O. 2006 The effect of coagulation with MF/UF membrane filtration for the removal of virus in drinking water. *J. Membr. Sci.* **279**(1–2), 364–371.

Jacangelo, J. G., Adham, S. S. & Laîné, J. M. 1995 Mechanism of cryptosporidium, Giardia, and MS2 virus removal by MF and UF. *J. AWWA.* **87**(9), 107–121.

Madaeni, S. S., Fane, A. G. & Grohmann, G. S. 1995 Virus removal from water and wastewater using membranes. *J. Membr. Sci.* **102**, 65–75.

Matsui, Y., Matsushita, T., Inoue, T., Yamamoto, M., Hayashi, Y., Yonekawa, H. & Tsutsumi, Y. 2003 Virus removal by ceramic membrane microfiltration with coagulation pretreatment. *Water Sci. Technol.: Water Supply.* **3**(5–6), 93–99.

Matsushita, T., Matsui, Y., Shirasaki, N. & Kato, Y. 2005 Effect of membrane pore size, coagulation time, and coagulant dose on virus removal by a coagulation-ceramic microfiltration hybrid system. *Desalination* **178**(1–3), 21–26.

Matsushita, T., Matsui, Y. & Shirasaki, N. 2006 Analyzing mass balance of viruses in a coagulation-ceramic microfiltration hybrid system by a combination of the polymerase chain reaction (PCR) method and the plaque forming units (PFU) method. *Water Sci. Technol.* **53**(7), 199–207.

Otaki, M., Yano, K. & Ohgaki, S. 1998 Virus removal in a membrane separation process. *Water Sci. Technol.* **37**(10), 107–116.

Urase, T., Yamamoto, K. & Ohgaki, S. 1996 Effect of structure of membranes and module configuration on virus retention. *J. Membr. Sci.* **115**, 21–29.

Zhu, B., Clifford, D. A. & Chellam, S. 2005*a* Virus removal by iron coagulation-microfiltration. *Water Res.* **39**, 5153–5161.

Zhu, B., Clifford, D. A. & Chellam, S. 2005*b* Comparison of electrocoagulation and chemical coagulation pretreatment for enhanced virus removal using microfiltration membranes. *Water Res.* **39**, 3098–3108.

First received 1 August 2007; accepted in revised form 22 November 2007

Parasitol Res (2008) 103:801–805
DOI 10.1007/s00436-008-1045-x

ORIGINAL PAPER

Occurrence of *Cryptosporidium* sp. in snakes in Japan

Toshiro Kuroki · Shinji Izumiyama · Kenji Yagita · Yumi Une · Hideki Hayashidani · Masaki Kuro-o · Akira Mori · Hajime Moriguchi · Michihisa Toriba · Toru Ishibashi · Takuro Endo

Received: 6 December 2007 / Accepted: 21 May 2008 / Published online: 13 June 2008

Abstract The aim of this study was to determine the prevalence of *Cryptosporidium* in snakes in Japan. Fecal samples or intestinal contents of 469 snakes, consisting of five species, were analyzed and *Cryptosporidium* oocysts were detected only from the Japanese grass snake *Rhabdophis tigrinus*. The mean prevalence of *Cryptosporidium* sp. in Japanese grass snakes was approximately 26% in the region studied. Histopathological observations revealed that the organism caused proliferative enteritis in the small intestine. Sequence analysis of a fragment of the small subunit rRNA gene has shown that the partial sequence of *Cryptosporidium* sp. isolated from the snakes was identical to that of the *Cryptosporidium* snake genotype W11 from New Guinea viper boa.

Introduction

The protozoan parasite, *Cryptosporidium*, has a wide range of vertebrate hosts from fish to mammals (Xiao et al. 2004a). In reptiles, two valid species, *C. serpentis* and *C. varanii*, were studied in depth. Recent analysis of *Cryptosporidium*

This study was supported by a Health Science Research Grant on Emerging and Re-emerging Infectious Diseases (15091601) from the Ministry of Health, Labor and Welfare, Japan. We thank many people who were involved in this study for providing snake samples.

T. Kuroki (✉)
Department of Microbiology,
Kanagawa Prefectural Institute of Public Health,
1-3-1 Shimomachiya,
Chigasaki, Kanagawa 253-0087, Japan
e-mail: kuroki.gcg3@pref.kanagawa.jp

S. Izumiyama · K. Yagita · T. Endo
Department of Parasitology, National Institute of Health,
1-23-1 Toyama,
Shinjuku-ku, Tokyo 162-8640, Japan

Y. Une
Department of Veterinary Pathology,
School of Veterinary Medicine, Azabu University,
1-17-71 Fuchinobe,
Sagamihara, Kanagawa 229-8501, Japan

H. Hayashidani
Institute of Symbiotic Science and Technology,
School of Veterinary Medicine,
Tokyo University of Agriculture and Technology,
3-5-8 Saiwai-cho,
Fuchu, Tokyo 183-8509, Japan

M. Kuro-o
Department of Biofunctional Science,
Faculty of Agriculture and Life Science, Hirosaki University,
3 Bunkyo-cho,
Hirosaki 036-8561, Aomori, Japan

A. Mori
Department of Zoology, Graduate School of Science,
Kyoto University,
Kitashirakawa-oiwake-cho, Sakyo,
Kyoto 606-8502, Japan

H. Moriguchi · M. Toriba
The Japan Snake Institute,
3318 Yabutuka-cho,
Ohta, Gunma 379-2301, Japan

T. Ishibashi
Inokashira-Koen Animal Hospital,
1-9-22 Shimorenjaku,
Mitaka, Tokyo 181-0013, Japan

genotypes revealed that there were several genotypes infecting reptiles (Xiao et al. 2004b). However, information such as host specificity, geographic distribution, and pathogenicity of other reptilian *Cryptosporidium* species are limited.

Contamination of *Cryptosporidium* oocysts in surface water or source water for drinking occurred worldwide (Hachich et al. 2004; Jiang et al. 2005; Payment et al. 2000; Xiao et al. 2000) and is of great concern for public health because oocysts are highly resistant to chlorination and are the causative agent of self-limiting diarrhea. The sources of *Cryptosporidium* are variable (Xiao et al. 2000; Jellison et al. 2002; Ward et al. 2002).

The contamination of *Cryptosporidium* in well water serving as the source of small community drinking water supply treated only with chlorination occurred in 2001 in Hyogo, the Kinki region, Japan (Tsuji et al. 2005). The drinking water supply was then stopped under the Japanese water regulations where delivery of water is prohibited when the contamination of *Cryptosporidium* is detected microscopically, regardless of the species or genotype. The DNA sequence of *Cryptosporidium* isolated was identical with those of AY120913, suggesting that the source of contamination was snakes. However, there has been limited information on *Cryptosporidium* from snake origin in Japan.

The aim of this study was to identify the source of *Cryptosporidium* from snakes and to investigate the prevalence of *Cryptosporidium* in native snakes in Japan. Samples from five snake species were analyzed and the small subunit (SSU) rRNA gene of *Cryptosporidium*-positive samples was characterized by DNA sequencing.

Material and methods

Collection of samples

A total of 469 snakes of five species, that is, Japanese grass snake (Yamakagashi) *Rhabdophis tigrinus*, Japanese rat snake (Aodaisho) *Elaphe climacophora*, Japanese four-striped rat snake (Shimahebi) *E. quadrivirgata*, Japanese forest rat snake (Jimuguri) *E. conspicillata*, and Mamushi *Gloydius blomhoffii*, were captured from different geographic locations (Table 1) between July 2001 and November 2007. They were kept separately in an enclosure usually for less than a week until fecal samples or intestinal contents were collected. Collected samples were stored at 4°C until used.

Analysis of *Cryptosporidium* oocysts

Detection of oocysts was performed by the direct smear method, followed by direct immunofluorescent staining. Approximately 0.5 g or less of intestinal contents or fecal samples were diluted twice with distilled water, mixed thoroughly, and filtered with double-sheeted gauze to remove large debris as needed. A small volume of suspension was smeared onto a slide glass, air dried for 30 min, and fixed with methanol. The direct immunofluorescent staining was performed with a commercial kit (FL-Crypt-a-Glo, Waterborne, New Orleans, LA, USA) and 4′-6-diamidino-2-phenylindole (DAPI) staining. The entire smear was examined at a magnification of ×200, and the sample was scored positive for *Cryptosporidium* if the suspected particle had fluorescein isothiocyanate (FITC) specific fluorescence with approximately 6×4 μm diameter and four DAPI positive nuclei.

DNA extraction and nested PCR

DNA was extracted with a QIAamp DNA stool mini kit (Qiagen). Nested polymerase chain reaction (PCR) was performed for sequence analysis of an approximately 850-base pair fragment from the small subunit rRNA gene on a PE 2400 thermal cycler (Perkin-Elmer), according to the method of Xiao et al. (2000) with a slight modification. Primers for the first PCR were 5′-TTC TAG AGC TAA TAC ATG CG-3′

Table 1 Prevalence of *Cryptosporidium* sp. in snakes by region in Japan

Region	No. of positive/no. analyzed				
	Japanese grass snake	Japanese four-striped rat snake	Japanese rat snake	Mamushi	Japanese forest rat snake
Hokkaido	–	0/1	–	–	0/5
Tohoku	11/27 (40.7%)	0/8	0/2	0/7	–
Kanto	6/43 (14.0%)	0/20	0/25	0/1	–
Shin-etsu/Hokuriku	4/4 (100%)	0/10	–	0/5	–
Tokai	0/2	0/7	0/5	–	–
Kinki	1/10 (10.0%)	0/79	0/6	–	–
Chugoku	31/101 (35.2%)	0/46	0/8	0/1	–
Shikoku	3/14 (21.4%)	0/5	–	0/1	0/1
Kyushu	1/22 (4.5%)	0/2	0/1	–	–
Total	57/223 (25.6%)	0/178	0/47	0/15	0/6

Fig. 1 Geographical location of the regions in Japan

and 5′-CCC ATT TCC TTC GAA ACA GGA-3′. The reaction mixture was 100 μl consisting of a 10 μl reaction buffer, 200 nM of each primer, 2 mM MgCl2, 0.2 mM of each deoxynucleoside triphosphate, 2.5 U Taq polymerase (ExTaq Hot start version, TakaraBio), and 1 μl of template DNA. A total of 40 cycles were carried out, each consisting of 94°C for 45 s, 55°C for 45 s, and 72°C for 1 min, with an initial hot start at 94°C for 5 min and a final extension at 72°C for 7 min. Primers for the second PCR were 5′-GGA AGG GTT GTA TTT ATT AGA TAA AG-3′ and 5′-AAG GAG TAA GGA ACA ACC TCC A-3′. The PCR conditions were identical to that of the first PCR.

DNA sequencing

PCR products of the 18S rRNA gene fragments were purified by using the QIAquick PCR purification kit (Qiagen) and sequenced on an ABI 310 automated sequencer (Applied Biosystems) using BigDye terminator cycle sequencing kit V1.1 (Applied Biosystems). Sequence accuracy was confirmed by two-directional sequencing of two separate PCR products. An alignment of sequences was compared by performing the Basic Local Alignment Search Tool.

Histopathological analysis

At necropsy after anesthesia, stomachs and intestines were fixed with 10% buffered neutral formalin, dehydrated, and embedded in paraffin. Histological sections were cut and stained with hematoxylin and eosin for examination by light microscopy.

Results

Fecal samples and/or intestinal contents were tested for the presence of *Cryptosporidium* oocysts from 469 snakes of five species. The oocysts were prevalent only in the Japanese grass snake *R. tigrinus* (Table 1), and none of the other four snakes species was positive for *Cryptosporidium*. Of the 223 Japanese grass snakes, 57(25.6%) were positive for *Cryptosporidium* sp. The regional prevalence of *Cryptosporidium* sp. among the snakes varied widely (Fig. 1) from 4.5% (one of 22) in Kyushu region to 100% (four of four) in Shin-etsu/Hokuriku region. *Cryptosporidium* was also detected in 11 of 27 snakes in Tohoku region, six of 43 snakes in Kanto region, one of ten snakes in Kinki

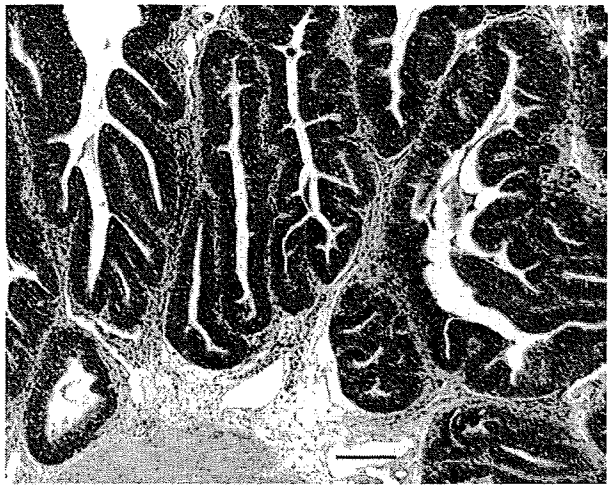

Fig. 2 Photograph of small intestinal mucosa from *R. tigrinus* with enteritis by *Cryptosporidium* sp. Note multilayered of epithelial cells and edema in the mucosal lamina propria. Hematoxylin–eosin stain. *Bar*=100 μm

region, 31 of 101 snakes in Chugoku region, and three of 14 snakes in Shikoku region.

One hundred and ten oocysts isolated from Japanese grass snakes measured 4.5–5.0×4.2–4.5 μm. They showed FITC specific fluorescence around the oocyst wall and DAPI specific fluorescence in four nuclei. Oocysts larger than 6 μm in length which is characteristic for gastric *Cryptosporidium* were not detected from snakes examined.

Sequence analysis of 18S rRNA fragment from 17 Japanese grass snakes throughout the country (Table 1) yielded DNA sequences identical to that of AY120913, which was originally isolated from New Guinea viper boa *Candoia asper* and designated as *Cryptosporidium* snake genotype W11 (Xiao et al. 2002, 2004a; Jiang et al. 2005; Feng et al. 2007).

Histopathological findings

Seven Japanese grass snakes positive for *Cryptosporidium* oocysts in the intestinal contents were examined for histopathological changes. On gross examination, the intestinal wall thickened in severe cases and retention of viscous fluid in the lumen of the small intestine were observed. On histological examination, pathological changes were limited to the small intestine. Intestinal lesions included scattered single cell necrosis of epithelial cells, loss of goblet cells, and edema in the mucosal lamina propria (Fig. 2). Stages of *Cryptosporidium* arranged in clusters and others dispersed on the apical brush border of the absorptive epithelial cells lining intestinal villi, where duplication, hyperplasia of epithelial cells were observed (Fig. 3). A few mononuclear inflammatory cells infiltrated the mucosal lamina propria.

Nucleotide sequence accession numbers

The nucleotide sequence of the SSU rRNA gene of *Cryptosporidium* sp. from Japanese grass snake has been deposited in GenBank under an accession no. AB222185.

Discussion

The prevalence of *Cryptosporidium* snake genotype W11 in the Japanese grass snake ranged from 4.5% to 100%, with the average of 25.6%. It is interesting to note that although experimental transmission of the *Cryptosporidium* snake genotype W11 was reported from five snake species of three different families by Xiao et al. (2004b), the infection was limited to the Japanese grass snake and did not occur even in the sympatric species, *E. climacophora* and *E. quadrivirgata*, that share habitat and diet (Fukada 1992). These three species are common snakes in Japan and belong to the family Colubridae.

Mild to severe enteritis in Japanese grass snakes with *Cryptosporidium* snake genotype W11 was observed in this study. A similar observation was made by Brower and Cranfield (2001) in 15 rough green snakes with *Cryptosporidium* associated enteritis and died 17 days after arrival in Baltimore Zoo. Prognosis of Japanese grass snakes with *Cryptosporidium* enteritis and impact on the natural snake population is to be examined.

It is of importance to note, from the public health point of view, that this reptilian species of *Cryptosporidium* may readily contaminate sources of drinking water, since the host snake is an inhabitant of waterfront areas and paddy

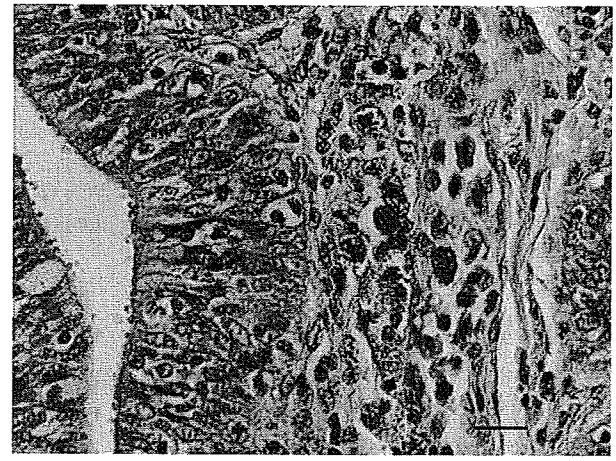

Fig. 3 Photograph of small intestinal mucosa from *R. tigrinus* with enteritis by *Cryptosporidium* sp. Note multilayered of epithelial cells, infiltration of mononuclear inflammatory cells are observed. Proliferative stages of *Cryptosporidium* are shown on the apical brush border of the absorptive epithelial cells. Hematoxylin–eosin stain. *Bar*= 20 μm

fields, and prey mainly on frogs (Kadowaki 1992). The oocyst is positive for immunostaining by the commercially available *Cryptosporidium* detection kit and is difficult to distinguish morphologically from those pathogenic to humans, such as *C. parvum* or *C. hominis*. According to the Japan water regulations, the water supply should be shut down immediately when *Cryptosporidium* oocyst of any species is detected microscopically in drinking water. Actually, a small drinking water plant in Hyogo, Japan was once forced to stop water supply due to contamination of a reptilian species of *Cryptosporidium* in 2001 (Tsuji et al. 2005), although there is no evidence that *Cryptosporidium* from snakes can cause cryptosporidiosis in humans. No patients of cryptosporidiosis were reported among residents who were served the water from the plant.

Interestingly, from the partial sequence analysis of rRNA gene, we found a single *Cryptosporidium* snake genotype W11 among wild snakes in Japan, while *C. serpentis* and *C. varanii* have often been isolated from imported reptiles such as corn snakes and leopard geckoes (Une et al. 2002, 2005). Thus far, no *Cryptosporidium* cases in native snakes have been found (Une, unpublished data). Results of our studies and clinical cases suggest that *C. serpentis* and *C. varanii* might occur quite rarely in domestic snakes in Japan.

References

Brower AI, Cranfield MR (2001) *Cryptosporidium*-associated enteritis without gastritis in rough green snakes (*Opheodrys aestivus*) and a common garter snake (*Thamnophis sirtalis*). J Zoo Wildl Med 32:101–105

Feng Y, Alderisio KA, Yang W, Blancero LA, Kuhne WG, Nadareski CA, Reid M, Xiao L (2007) *Cryptosporidium* genotypes in wildlife from a New York watershed. Appl Environ Microbiol 73:6475–6483

Fukada H (1992) Snake life history in Kyoto. Impact Shuppankai, Tokyo, p 172

Hachich EM, Sato MI, Galvani AT, Menegon JR, Mucci JL (2004) *Giardia* and *Cryptosporidium* in source waters of Sao Paulo State, Brazil. Water Sci Technol 50:239–245

Jellison KL, Hemond HF, Schauer DB (2002) Sources and species of *Cryptosporidium* oocysts in the Wachusett Reservoir watershed. Appl Environ Microbiol 68:569–575

Jiang J, Alderisio KA, Xiao L (2005) Distribution of *Cryptosporidium* genotypes in storm event water samples from three watersheds in New York. Appl Environ Microbiol 71:4446–4454

Kadowaki M (1992) Food resource overlap between the two sympatric Japanese snakes (*Elaphe quadrivirgata* and *Rhabdophis tigrinus*) in the paddy fields. Jpn J Ecol 42:1–7

Payment P, Berte A, Prevost M, Menard B, Barbeau B (2000) Occurrence of pathogenic microorganisms in the Saint Lawrence River (Canada) and comparison of health risks for populations using it as their source of drinking water. Can J Microbiol 46:565–576

Tsuji H, Oshibe T, Ono K, Yamamoto S, Chikahira M, Masuda K, Yagita K, Izumiyama S, Endo T, Yamaoka M (2005) Detection of *Cryptosporidium* derived from reptile in the source water of a public simple water supply, Hyogo Prefecture. Bull Hyogo Prefect Inst Public Health Environ Sci 2:10–17

Une Y, Kuroki T, Endo T, Suzuki T, Ishibashi T, Ishikawa T (2002) Epidemiology and pathology of cryptosporidiosis in lizards. The 134th general meeting of the Japanese Society of Veterinary Science, sppl WS-077

Une Y, Ishibashi T, Nomura Y (2005) Cryptosporidiosis in snakes. The 4th workshop of the Society for Care and Pathology on Reptiles and Amphibians. suppl P-14

Ward PI, Deplazes P, Regli W, Rinder H, Mathis A (2002) Detection of eight *Cryptosporidium* genotypes in surface and waste waters in Europe. Parasitology 124(Pt 4):359–368

Xiao L, Alderisio K, Limor J, Royer M, Lal AA (2000) Identification of species and sources of *Cryptosporidium* oocysts in storm waters with a small-subunit rRNA-based diagnostic and genotyping tool. Appl Environ Microbiol 66:5492–5498

Xiao L, Sulaiman IM, Ryan UM, Zhou L, Atwill ER, Tischler ML, Zhang X, Fayer R, Lal AA (2002) Host adaptation and host–parasite co-evolution in *Cryptosporidium*: implications for taxonomy and public health. Int J Parasitol 32:1773–1785

Xiao L, Fayer R, Ryan U, Upton SJ (2004a) *Cryptosporidium* taxonomy: recent advances and implications for public health. Clin Microbiol Rev 17:72–97

Xiao L, Ryan UM, Graczyk TK, Limor J, Li L, Kombert M, Junge R, Sulaiman IM, Zhou L, Arrowood MJ, Koudela B, Modry D, Lal AA (2004b) Genetic diversity of *Cryptosporidium* spp. in captive reptiles. Appl Environ Microbiol 70:891–899

(8-6)環境水中の原虫類検出を目的としたLAMP法の検討

○猪又　明子(東京都健康安全研究センター)　保坂　三継(東京都健康安全研究センター)
泉山　信司(国立感染症研究所)　百田　隆祥(特別会員)
大谷喜一郎(神奈川県内広域水道企業団)　遠藤　卓郎(国立感染症研究所)

1．はじめに

水中の原虫類（クリプトスポリジウム，ジアルジア）の検出は，試料水を濃縮，精製後に蛍光抗体染色を行い，顕微鏡観察により行っている。しかし，顕微鏡観察には熟練が必要であり，検査に長時間かかる等の問題点がある。

そこで，より簡便で迅速な検査法として，クリプトスポリジウムおよびジアルジアを対象としたLAMP法を開発した。LAMP法の実用性を評価するために，種々の環境水（河川水，湖沼水，湧水等）を用いて原虫類を検査し，検鏡法による結果と比較，検討した。

2．材料と方法

2.1 供試水

東京都内および神奈川県内の環境水17検体を検査した。内訳は，湖沼水（貯水池を含む）3検体，河川水10検体，湧水4検体である。検査水量は，検鏡法，LAMP法とも10Lとした。

2.2 検査方法

試料水をろ過濃縮した後，捕捉物を剥離し，免疫磁気ビーズにより捕捉した。

検鏡法用の検体は，磁気ビーズ捕捉後に塩酸添加回収を3回行い，100℃で5分間加熱処理後にDAPI染色および直接蛍光抗体染色を行った。落射蛍光顕微鏡によるクリプトスポリジウムオーシストおよびジアルジアシストの大きさ，形，核の観察と，微分干渉像による内部構造の観察により判定を行い，(オー)シスト数を計数した。(オー)シストの判定基準は「水道における指標菌及びクリプトスポリジウム等の検査方法について（厚生労働省　健水発第0330006号，平成19年3月30日)」に従った。

LAMP用の検体は，磁気ビーズ捕捉後に上澄みを除去し，凍結融解（-80℃，37℃）を5回繰り返して(オー)シストを破壊した。DNA抽出はプロテイナーゼK/DTT添加後60℃20分間のインキュベートにより行った。さらに超音波処理を行い，75℃10分間，95℃5分間のインキュベート後に，反応チューブ1本当たり5μLずつDNA抽出物を添加し，LAMP反応を行った。LAMPは63℃で1時間反応させ，クリプトスポリジウム及びジアルジアについて陰性，陽性を判定した。

LAMP法で陽性となった検体等については，残ったDNA抽出物を再度LAMP検査するとともに，LAMP増幅産物を制限酵素で切断後，陽性対照と比較を行った。

3．結果

3.1 クリプトスポリジウム

検鏡法，LAMP法とも，17検体全てクリプトスポリジウム不検出であった。

3.2 ジアルジア

検鏡法では，河川水1検体（検体A）からジアルジアが2シスト/10L検出された。その他の16検体は不検出であった。

LAMP 法では，検鏡法でジアルジアが検出された河川水（検体 A）及び湧水 1 検体（検体 B）が陽性となった。また，湖沼水 1 検体（検体 C）では，判定は陰性となったものの，LAMP 反応による濁度上昇が見られた。

検体 A，B，C について，残った DNA 抽出物を再度 LAMP 検査した結果を図 1 に示した。検体 A-1，A-2，B は陽性対照（PC）と同様の濁度増加を示したが，検体 C では濁度増加が見られなかった。これは，再検査前に誤って UV 照射を行ったことにより，検体 C の遺伝子が破壊されたためと考えられる。

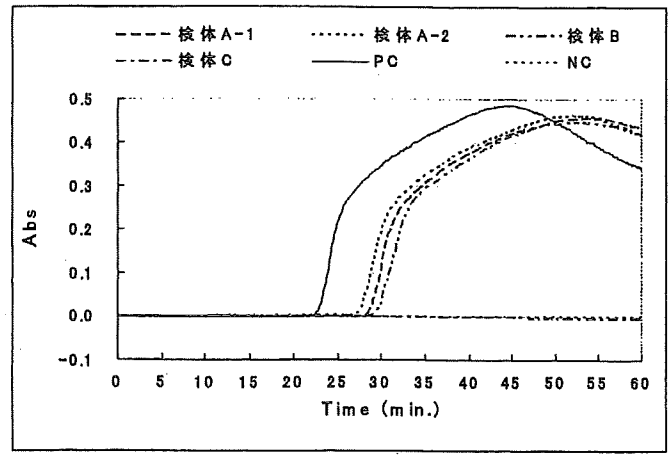

図 1　ジアルジア LAMP 再検査結果

LAMP による産物がジアルジアの DNA であることを確認するために，検体 A, B, C の LAMP 産物及び図 1 に示した検体 A-1，A-2，B の LAMP 産物を制限酵素（*Ban* II）で切断し，ジアルジア陽性対照と比較した（図 2）。全ての LAMP 産物がジアルジアと一致したことから，検体 A,B,C はジアルジア陽性であることが確認できた。

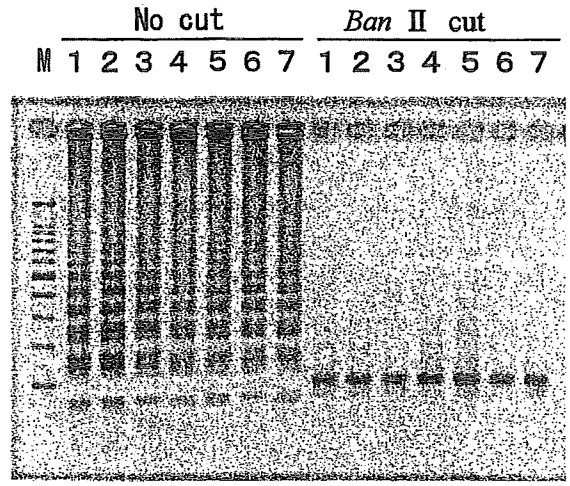

図 2　LAMP 産物の解析

4．考察

今回検査した 17 検体の環境水について，クリプトスポリジウムは検鏡法，LAMP 法とも全て不検出であったことから，LAMP 法の誤陽性は認められなかった。ジアルジアでは，検鏡法で検出された検体が LAMP 法でも陽性となったことから，誤陰性は認められなかった。検鏡法で不検出であった 2 検体がジアルジア陽性であることが LAMP 法 により明らかになった。しかし，このうち 1 検体は LAMP 増幅産物により濁度が増加したものの，陰性と判定された。現在の判定条件は暫定条件であることから，より正確な判定となるよう設定値を検討する必要がある。

このような問題点はあるものの，LAMP 法が検鏡法よりも高感度である可能性が示された。この理由として，検鏡法では磁気ビーズ捕捉後に原虫類をビーズから解離して染色を行うのに対し，LAMP 法では磁気ビーズに捕捉された原虫類から直接 DNA 抽出を行うために解離時のロスがないことが考えられる。

クリプトスポリジウムの検出感度については，今後さらに多くの環境水を用いて評価する必要がある。

Chemosphere 73 (2008) 1724–1730

Contents lists available at ScienceDirect

Chemosphere

journal homepage: www.elsevier.com/locate/chemosphere

Formation of *N*-nitrosodimethylamine (NDMA) by ozonation of dyes and related compounds

Masami Oya [a,1], Koji Kosaka [a,*], Mari Asami [a], Shoichi Kunikane [b]

[a] Department of Water Supply Engineering, National Institute of Public Health, 2-3-6 Minami, Wako, Saitama 351-0197, Japan
[b] Institute for Environmental Sciences, University of Shizuoka, 52-1 Yada, Suruga-ku, Shizuoka 422-8526, Japan

ARTICLE INFO

Article history:
Received 17 May 2008
Received in revised form 9 September 2008
Accepted 9 September 2008

Keywords:
N-nitrosodimethylamine
Dye
Ozone
Hydroxyl radical

ABSTRACT

Formation of *N*-nitrosodimethylamine (NDMA) by ozonation of commercially available dyes and related compounds was investigated. Ozonation was conducted using a semi-batch type reactor, and ozone concentration in gas phase and the ozone gas flow were 10 mg L^{-1} and 1.0 L min^{-1}, respectively. NDMA was formed by 15 min of ozonation of seven out of eight selected target compounds (0.05 mM) at pH 7. All the target compounds with *N,N*-dimethylamino functions were NDMA precursors in ozonation. The lowest and highest NDMA concentrations after ozonation of the target compounds were 13 ng L^{-1} for *N,N*-dimethylformamide (DMF) and 1600 ng L^{-1} for *N,N*-dimethyl-*p*-phenylenediamine (DMPD), respectively. NDMA concentrations after 15 min of ozonation of 0.05 mM methylene blue (MB) and DMPD increased with an increase in pH in its range of 6–8. The effects of coexisting compounds on NDMA concentrations after 15 min of ozonation of 0.05 mM MB and DMPD were examined at pH 7. NDMA concentrations after ozonation of MB and DMPD increased by the presence of 0.05 mM (0.7 mg L^{-1} as N) nitrite (NO_2^-); 5000 ng L^{-1} for MB and 4000 ng L^{-1} for DMPD. NDMA concentration after MB ozonation decreased by the presence of 5 mM *tertiary* butyl alcohol (TBA), a hydroxyl radical (HO·) scavenger, but that after DMPD ozonation was increased by the presence of TBA. NDMA concentrations after ozonation of MB and DMPD were not affected by the presence of 0.16 mM (5.3 mg L^{-1}) hydrogen peroxide (H_2O_2). When 0.05 mM MB and DMPD were added to the Yodo and Tone river water samples, NDMA concentrations after 15 min of their ozonation at pH 7 increased compared with those in the case of addition to ultrapure water samples.

1. Introduction

N-Nitrosodimethylamine (NDMA) is a type of nitrosamines classified as potent carcinogens (United States Environmental Protection Agency (US EPA), 1993a,b). According to the Integrated Risk Information System of US EPA (1993b), NDMA concentration in drinking water associated with an excess lifetime carcinogenic risk of 10^{-5} is 7 ng L^{-1}. In January 2007, six nitrosamines were selected from the contaminants in the second Unregulated Contaminant Monitoring Regulation by US EPA (2007). In February 2008, five nitrosamines were selected from the contaminants in the third Contaminant Candidate List by US EPA (2008). NDMA is included in both lists as one of the nitrosamines. The drinking water standard for NDMA known as the maximum contaminant level has not yet been established in the US. However, the notification level for NDMA has already been established at 10 ng L^{-1} in California (California Department of Public Health).

Since the detection of NDMA in drinking water, the occurrence of NDMA in water treatment plants (WTPs) has been investigated, mainly in the US and Canada (Barrett et al., 2003; California Department of Public Health; Charrois et al., 2007). NDMA was found to be formed by chloramination or chlorination in the presence of ammonia, so the occurrence of NDMA in sewage treatment plants (STPs) has also been investigated (Najm and Trussell, 2001; Mitch et al., 2003). Moreover, the occurrence and identification of NDMA precursors and the NDMA formation mechanisms in chloramination or chlorination have also been studied by several researchers (Gerecke and Sedlak, 2003; Mitch et al., 2003; Mitch and Sedlak, 2004; Chen and Valentine, 2006; Chen and Valentine, 2007).

On the other hand, regarding ozonation, studies conducted relating to NDMA were mainly on its reduction rather than on its formation as oxidation by-product. For example, it was reported that reaction rate constants of NDMA with ozone and hydroxyl radical (HO·) were $(5.2 \pm 0.16) \times 10^{-2}$ and $(4.5 \pm 0.21) \times 10^{8}$ M^{-1} s^{-1}, respectively, and NDMA were dominantly

* Corresponding author. Tel. +81 48 458 6306; fax: +81 48 458 6305.
E-mail address: kosaka@niph.go.jp (K. Kosaka).
[1] Current address: Water Supply Division, Health Bureau, Ministry of Health, Labor and Welfare, 1-2-2 Kasumigaseki, Chiyoda-ku, Tokyo 100-8916, Japan.

0045-6535/$ - see front matter © 2008 Elsevier Ltd. All rights reserved.
doi:10.1016/j.chemosphere.2008.09.026

decomposed by HO· during ozonation (Lee et al., 2007b). Lee et al. (2007a) reported that when selected NDMA precursors were preozonated, the NDMA formation potentials by chloramination were decreased. More recently, however, several studies of NDMA formation by ozonation have been reported. Andrzejewski et al. (2008) reported that NDMA is formed by dimethylamine (DMA) ozonation. Another study (Schmidt and Brauch, 2008) showed that a plant growth regulator, daminozide, its decomposition product (i.e., 1,1-dimethylhydrazine), a fungicide, tolyfluanide, and its decomposition products (i.e., *N,N*-dimethyl-*N'*-*p*-tolylsulphamide and dimethylsulfamide) are NDMA precursors in ozonation.

Furthermore, it was reported that NDMA of approximately 10 to approximately 100 ng L^{-1} was formed in ozonation in WTPs whose raw water came from the Yodo river, although the amount of NDMA formed was effectively decreased by a biological activated carbon process (Tateishi et al., 2008; Asami et al., submitted for publication). In our previous study (Oya et al., 2008b), we reported that NDMA precursors in ozonation in the Yodo river originated from the effluent of STPs located upstream. We also reported that NDMA was formed by ozonation in one of the STPs located upstream of the Yodo river, and that a high NDMA formation potential by ozonation originated from a STP influent which was colored solution and contained effluents from dye industries. However, there is as yet no information on NDMA formation by ozonation of dyes and related compounds. Water from the Yodo river is used as raw water in WTPs in the west part of Japan and total population supplied with water by these WTPs is more than 10 million. In addition, ozonation is often applied to wastewater treatments for the purposes of color removal. Therefore, it is important to determine the relationship between ozonation and NDMA formation from dyes and related compounds.

In this study, NDMA formation by ozonation of selected dyes and related compounds was investigated. We focused on the effects of reaction time, pH and coexisting compounds. Moreover, NDMA formation by the ozonation of target compounds added to river water samples was also investigated.

2. Methods

2.1. Reagents and solutions

Many synthetic dyes are used in Japan. For example, there are more than 1300 dyes categorized as disperse dye, a dye group whose productions are the largest in Japan, on the market (The Chemical Daily, 2006a). Various agents such as dispersants are also used for dyeing. Among these compounds, eight target compounds (methylene blue (MB, purity, >98.5%), methyl orange (MO), methyl violet B (MVB), auramine (purity, >80%), brilliant green (BG), *N,N*-dimethylformamide (DMF, purity, >99.5%), *N,N*-dimethylaminobenzene (DMAB, purity, >99%) and *N,N*-dimethyl-*p*-phenylenediamine (DMPD, purity, >98%)) were selected as target compounds in this study. The chemical structures of NDMA and these target compounds are shown in Fig. 1. The reagents of the target compounds were commercially obtained from Wako Pure Chemicals (Osaka, Japan), except for DMPD (Tokyo Chemical Industry, Tokyo, Japan). No purity data of MO, MVB and BG were obtained. The target compounds are selected to have *N,N*-dimethylamino functions, except BG having *N,N*-diethylamino functions. This is because compounds with *N,N*-dimethylamino functions were NDMA precursors in ozonation (Andrzejewski et al., 2008; Schmidt and Brauch, 2008). MB, MO, MVB, auramine and BG are dyes. DMF and DMAB were also selected because they are used as the synthetic intermediates of dyes (The Chemical Daily, 2006b). DMPD is not a synthetic intermediate of dyes, but it was selected because it is DMAB added with an amino function. The regents of the target compounds were used without further purification. However, in case of MO regent, it was purified using high-performance liquid chromatography (HPLC, HP1100 series, Agilent Technologies, Palo Alto, California, USA) and also used. NDMA standard solution was purchased from Supelco (Bellefonte, Pennsylvania, USA). NDMA-d_6, a surrogate of NDMA, was purchased from C/D/N Isotopes (Pointe-Claire, Canada). Ultrapure water used was purified with a Gradient A10 water purification system (Millipore, Bedford, Massachusetts, USA). River water samples were collected from the Yodo and Tone rivers in February 2008 and stored in the dark at 4 °C. Both Yodo and Tone river waters were used as raw water for WTPs. As described above, NDMA precursors in ozonation were present in the Yodo river water samples (Asami et al., submitted for publication). The basic water quality of these river water samples is shown in Supplementary material (Table S1).

2.2. Ozonation experiments of target compounds

Ozonation experiments were conducted using a glass bottle as a semi-batch-type reactor. The sample volume was 1 L and reaction temperature was 20 °C. Ozone gas was generated by an ozone generator (POX-20, Fuji Electric, Tokyo, Japan) using pure oxygen. The experiments were started by bubbling ozone gas into a reactor. The ozone concentration in gas phase was 10 mg L^{-1} and the ozone gas flow rate was 1.0 L min^{-1}. Other basic ozonation conditions were as follows: initial (added) concentration of target compounds, 0.05 mM; pH of samples, 7 (5 mM phosphate-buffered solution); and reaction time, 15 min. For the ozonation experiment of MO purified, initial MO concentration was 0.025 mM and reaction time was 7.5 min. MO unpurified was also ozonated under the same conditions. When the effect of reaction time on NDMA formation by ozonation of target compounds was investigated, the reaction times ranged from 3.5 to 15 min. When the effect of the pH of the samples on NDMA formation by ozonation of the target compounds was investigated, the pHs of the samples ranged from 6 to 8 (5 mM phosphate-buffered solution). When the effects of coexisting compounds and river water matrix on NDMA formation by the ozonation of target compounds were investigated, sodium nitrite ($NaNO_2$, Aldrich, Saint Louis, Missouri, USA), *tertiary* butyl alcohol (TBA, Wako Pure Chemicals, Osaka, Japan), hydrogen peroxide (H_2O_2, Wako Pure Chemicals, Osaka, Japan), and Yodo and Tone river water samples were used. The concentrations of NO_2^-, TBA and H_2O_2 added were 0.05 mM (0.7 mg L^{-1} as N), 5 mM and 0.16 mM (5.3 mg L^{-1}), respectively. The river water samples were filtered (GF/F, Whatman, Florham Park, New Jersey, USA) before use. When the effects of the concentrations of target compounds added on NDMA formation by ozonation were investigated using river water samples, their initial concentrations were 0.0005 and 0.05 mM. After each experiment, dissolved ozone in the sample was quenched by sodium thiosulfate (Wako Pure Chemicals, Osaka, Japan).

2.3. Analysis

The NDMA concentrations of samples were determined using solid-phase extraction (SPE) followed by ultra-performance liquid chromatography (UPLC, ACQUITY UPLC system, Waters, Milford, Massachusetts, USA) coupled with tandem mass spectrometry (MS/MS, ACQUITY TQD, Waters, Milford, Massachusetts, USA). Its analytical method was the same as those of our previous studies (Oya et al., 2008a; Asami et al., submitted for publication) and is briefly described in Supplementary material including Table S2. The sample volume for SPE was 100 mL, except in experiments using river water samples, where the sample volume was 500 mL. Smaller sample volumes for SPE were applied when NDMA concentrations were considered high. The multiple reaction

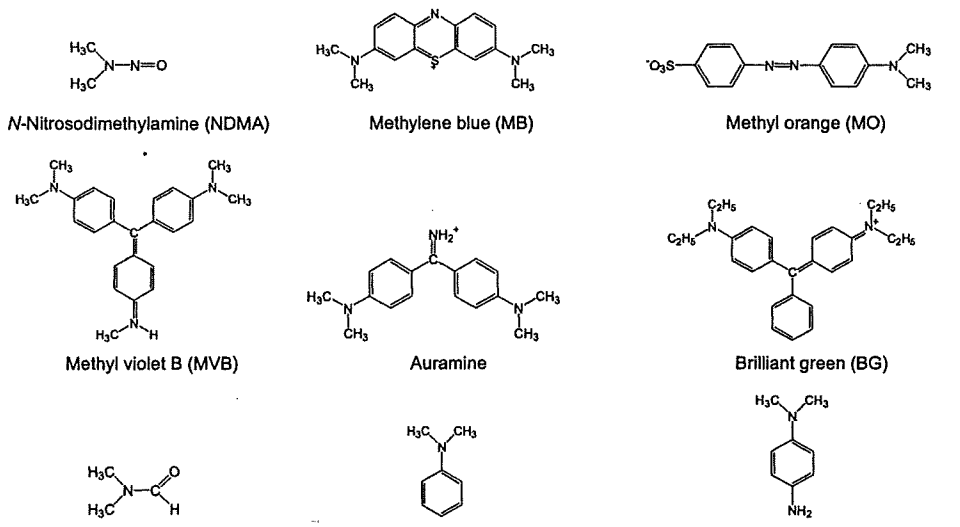

Fig. 1. Chemical structures of NDMA and target compounds.

monitoring (MRM) transitions were *m/z* 74.9–43.1 (quantification) and *m/z* 74.9–57.9 (confirmation) for NDMA, and *m/z* 81.0–46.0 for NDMA-d_6. The method detection limit (MDL) for NDMA was 5.0 ng L^{-1}, except in the cases using river water samples (MDL for NDMA, 1.0 ng L^{-1}).

For target compounds, the decompositions of dyes were evaluated based on their colors. The color of a dye was measured by optical density at a wavelength of their maximum absorbance, that is, 665 nm for MB, 465 nm for MO, 584 nm for MVB, 431 nm for auramine and 625 nm for BG. Dissolved organic carbon (DOC) concentration was determined using a TOC analyzer (TOC-V CPH, Shimadzu, Kyoto, Japan). Total dissolved nitrogen (TDN) concentration was determined by spectrophotometry with peroxodisulfate decomposition (Japan Water Works Association, 2001). Ammonia (NH_3) concentration was determined by spectrophotometry using an indophenol method (Japan Water Works Association, 2001). Nitrate (NO_3^-) and NO_2^- concentration by ion chromatography (DX-500, Dionex, Sunnyvale, California, USA). Dissolved organic nitrogen (DON) concentration was calculated by subtracting NH_3, NO_3^- and NO_2^- concentrations from TDN concentration. Ozone concentration in gas phase was measured using an ultraviolet (UV) meter (PG-620HA, Ebara Jitsugyo, Tokyo, Japan).

3. Results and discussion

3.1. Difference according to target compounds

Table 1 shows NDMA concentrations after the ozonation of eight selected target compounds. NDMA concentration before the ozonation of all the selected target compounds was less than its MDL (5.0 ng L^{-1}). NDMA was formed by the ozonation of seven out of eight selected target compounds at pH 7. NDMA was detected after the ozonation of all the target compounds with *N,N*-dimethylamino functions.

The lowest and highest NDMA concentrations after the ozonation of target compounds were 13 ng L^{-1} for DMF and as high as 1600 ng L^{-1} for DMPD, respectively. Excluding BG, the value of a transformation factor of the target compounds for NDMA formation in ozonation (*F*) expressed by Eq. (1) was in the range of 3.5×10^{-4}–4.3×10^{-2}% (Table 1).

Table 1
NDMA concentrations after the ozonation of target compounds[a]

Target compound	Decomposition rate (%)[b]	NDMA concentration (ng L^{-1})[c]	*F* (%)[d]
MB	96	310	8.3×10^{-3}
MO	99	270	7.2×10^{-3}
MVB	92	460	1.2×10^{-2}
Auramine	96	480	1.3×10^{-2}
BG	99	<MDL (5.0)	$<1.0 \times 10^{-4}$
DMF	-	13	3.5×10^{-4}
DMAB	-	240	6.4×10^{-3}
DMPD	-	1,600	4.3×10^{-2}

[a] Ozonation conditions: initial concentration of target compounds, 0.05 mM; reaction time, 15 min; pH, 7 (5 mM phosphate-buffered solution); temperature, 20 °C.
[b] Decomposition rate was evaluated from the change in color.
[c] NDMA concentrations before ozonation of all the samples were less than the MDL (5.0 ng L^{-1}).
[d] Percentage of transformation factor for NDMA formation in ozonation of target compound (see Eq. (1)).

$$F(\%) = 100\frac{[\mathrm{NDMA}]}{[\mathrm{M}]_0} \quad (1)$$

where [NDMA] (M) is NDMA concentration after ozonation and $[M]_0$ (M) is the initial concentration of a target compound. The maximum *F* value of DMA at pH 7.5 was about 1.0×10^{-2}%, which was estimated from the figure of the previous paper (Andrzejewski et al., 2008) by the authors. Schmidt and Brauch (2008) reported that the *F* values of daminozide, tolyfluanide and their decomposition products added to nonchlorinated drinking water at pH 7.4 were 9–80%. It should be noted that no NDMA was formed by DMA ozonation in this study. The reason for such a discrepancy between the two studies might be that initial (added) DMA concentrations in the study of Andrzejewski et al. (2008), 30–700 mg L^{-1}, were much higher than that in the study of Schmidt and Brauch (2008), 2 μg L^{-1}, so NDMA formed was detected in the study of Andrzejewski et al. (2008). Thus, some *F* values in our study were higher than that of DMA, but all *F* values in our study were much lower than those of daminozide, tolyfluanide and their decomposition products. In the case of dyes (i.e., MB, MO, MVB, auramine and BG), their decompositions by ozonation ranged from 92% to 99%, as evaluated from the changes in their colors (Table 1). Of the three remaining

compounds, DMF is not reactive with ozone, but DMAB is reactive with ozone (the reaction rate constants of DMF and DMAB with ozone are 0.24 and $2.0 \times 10^9\ M^{-1}\ s^{-1}$, respectively (Lee et al., 2007a)). DMPD is also considered reactive with ozone because DMPD is DMAB added with an amino function, a reactive function with ozone (Neta et al., 1988). Thus, it was considered that all target compounds, except DMF, decomposed in ozonation.

The target compounds have one or two *N,N*-dimethylamino functions, except BG. However, NDMA formations by ozonation of the target compounds had no correlation with the number of *N,N*-dimethylamino functions in their molecules. At present, the mechanism of NDMA formation by ozonation is unclear; however, it is considered that the presence and association of *N,N*-dimethylamino functions may be required for NDMA formation. As described above, the NDMA formation by DMPD ozonation was the highest, although the number of *N,N*-dimethylamino functions of DMPD is only one and the difference of chemical structures between DMPD and DMAB is only an amino function of DMPD. Therefore, it was presumed that an amino function of DMPD might effectively act as the source of a nitroso function of NDMA in ozonation.

The remaining one target compound, BG, has *N,N*-diethylamino functions. Considering the results of other target compounds, it was thought that *N*-nitrosodiethylamine (NDEA) might be formed by BG ozonation. NDEA concentration in drinking water with an excess lifetime carcinogenic risk of 10^{-5}, 2 ng L^{-1} (US EPA, 1993a), is lower than NDMA concentration, 7 ng L^{-1} (US EPA, 1993b). Thus, NDMA evaluation as well as NDEA evaluation was considered to be important although NDEA was not investigated in this study.

It is known that dyes generally contain impurities. In case of this study, except for MB, the purities of dyes (i.e., MO, MVB, auramine and BG) are unknown or not so high, but all of them were used without purification. However, NDMA was detected after ozonation of DMAB (purity, >99%), a basic structural compound of the dyes with *N,N*-dimethylamino functions investigated. Moreover, MO was purified and ozonated (initial MO concentration, 0.025 mM; reaction time, 7.5 min). NDMA was detected at 51 ng L^{-1} after ozonation of MO purified. Before its ozonation, NDMA was not detected. Therefore, it was confirmed that dyes and related compounds with *N,N*-dimethylamino functions were NDMA precursors by ozonation. Of course, the impurities of target compounds might also contribute to NDMA formation during ozonation, particularly for dyes. However, in case of MO reagent, MO was main NDMA precursor by ozonation because NDMA concentration after ozonation of MO unpurified, 47 ng L^{-1}, was similar to that of MO purified under the same ozonation conditions (initial MO concentration, 0.025 mM; reaction time, 7.5 min).

3.2. Effects of reaction time, pH and coexisting compounds

Fig. 2 shows profiles of NDMA concentration and color removal during the ozonation of MB and DMPD. MB was selected because, three out of the four selected dyes with *N,N*-dimethylamino functions, no purity data of MO or MVB were obtained and the purity of MB was much higher than that of auramine. DMPD was selected because it was the strongest NDMA precursor in ozonation of the target compounds. In Fig. 2, color was measured for only MB because DMPD was colorless before ozonation. However, DMPD turned purple-red after ozone gas introduction. After that, the color gradually decreased and became colorless again until 15 min. NDMA concentrations by the ozonation of MB and DMPD increased with reaction time up to 15 min. In this study, the reaction time of ozonation was basically 15 min. Thus, it was clear from this result that NDMA would be formed from MB and DMPD by ozonation under the conditions employed in this study.

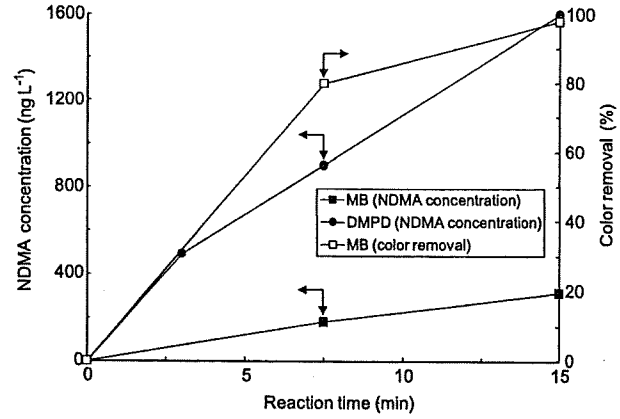

Fig. 2. Profiles of NDMA concentration and color removal during the ozonation of MB and DMPD. Ozonation conditions: initial concentration of target compounds, 0.05 mM; pH, 7 (5 mM phosphate-buffered solution); temperature, 20 °C.

Fig. 3 shows the effect of pH on NDMA formation by the ozonation of MB and DMPD. NDMA concentrations before ozonation were less than its MDL (5.0 ng L^{-1}) at all pH. NDMA concentrations after the ozonation of MB and DMPD ranged depending on pH from 150 to 1200 ng L^{-1} and 1100 to 5000 ng L^{-1}, respectively. That is, for both MB and DMPD, NDMA formation was enhanced with pH increase. It was reported that in a pH range of 6.5–10.5, NDMA formation by DMA ozonation increased with pH as well (Andrzejewski et al., 2008). That is, the result of this study agreed with that of the previous study. Ozone absorption rates during ozonation of MB and DMPD gradually decreased with time, but were not affected by pH (Figure S1). At 15 min of reaction time, ozone absorption rates of MB ozonation at pH 6–8 were 27–28% and those of DMPD at pH 6–8 were 25–26%. Thus, it was considered that the effects of pH on the NDMA formation by the ozonation of target compounds were not due to the difference of ozone consumption but due to the difference of reaction mechanism among pH 6–8.

Fig. 4 shows the effects of coexisting compounds on NDMA formation by the ozonation of MB and DMPD. Except in the case of NO_2^-, NDMA concentration before the ozonation of MB and DMPD in the presence of coexisting compounds were less than the MDL (5.0 ng L^{-1}). NDMA concentrations before the ozonation of target compounds in the presence of NO_2^- were 11 ng L^{-1} for MB and 68 ng L^{-1} for DMPD. No NDMA was detected in a NO_2^- solution.

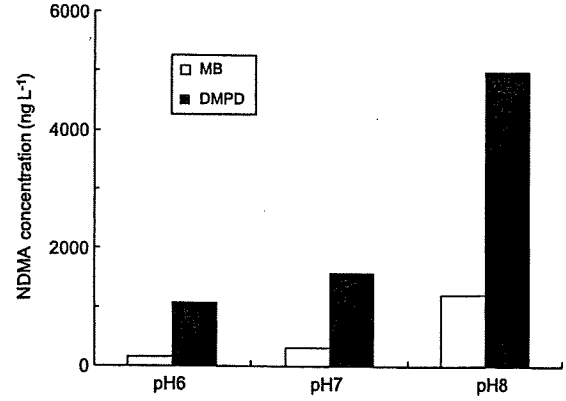

Fig. 3. Effects of pH on NDMA concentration after the ozonation of MB and DMPD. Ozonation conditions: initial concentration of target compounds, 0.05 mM; reaction time, 15 min; pH, 6–8 (5 mM phosphate-buffered solution); temperature, 20 °C. NDMA concentrations before ozonation, <MDL (5.0 ng L^{-1}).

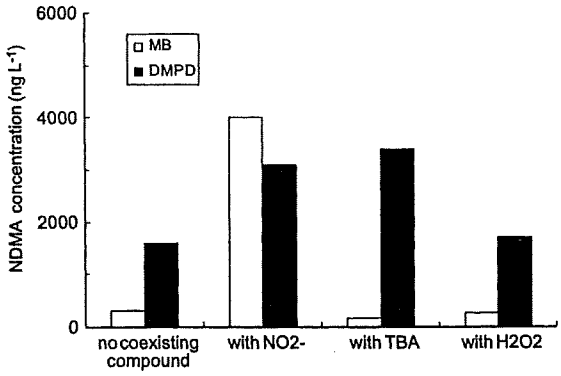

Fig. 4. Effects of coexisting compounds on NDMA concentration after the ozonation of MB and DMPD. Ozonation conditions: initial concentration of target compounds, 0.05 mM; initial concentrations of coexisting compounds, 0.05 mM (0.7 mg L^{-1} as N) NO_2^-, 5 mM TBA and 0.16 mM (5.3 mg L^{-1}) H_2O_2; reaction time, 15 min; pH, 7 (5 mM phosphate-buffered solution); temperature, 20 °C. NDMA concentrations before ozonation (except in the presence of NO_2^-), <MDL (5.0 ng L^{-1}). NDMA concentrations before ozonation in the presence of NO_2^-, 11 ng L^{-1} for MB and 68 ng L^{-1} for DMPD.

To investigate NDMA detection in the presence of NO_2^-, additional experiments were conducted with other target compounds at pH 7 (5 mM phosphate-buffered solution). In case of 0.05 mM auramine, 0.025 mM MO unpurified and 0.025 mM MO purified, NDMA was not detected in the presence of 0.05 mM NO_2^-. Also, in case of 0.05 mM DMAB (purity, >99%), NDMA was not detected in the presence of 0.05 mM NO_2^-, although DMAB is a basic structural compound in the target compounds investigated. The reason of the NDMA detections in the mixtures of some target compounds (i.e., MB and DMPD) and NO_2^- was unclear in this study. However, it was thought that NDMA might be formed by the reaction of the reagents of the target compounds with NO_2^-. So far, in case of DMA, it is known that NDMA is formed by the reaction of DMA and NO_2^-. Choi and Valentine (2002) reported that NDMA was formed at about 2 μg L^{-1} by the reaction of 0.1 mM DMA and 0.1 mM NO_2^- at pH 7.0 ± 0.1 (1 mM bicarbonate-buffered solution). Also, Lv et al. (2007) theoretically investigated with mathematical model and reported that NDMA was formed by the reaction of DMA and NO_2^- in the presence of carbon dioxide, a catalyst. It was thought that like the case of DMA, such catalysts might be required for the NDMA formation in the case of this study.

NDMA concentration after MB ozonation in the absence of NO_2^- was 310 ng L^{-1}, while that in the presence of NO_2^- was 4000 ng L^{-1}. It should be noted that no NDMA was formed by NO_2^- ozonation. Thus, NDMA concentration after MB ozonation markedly increased by the presence of NO_2^-. As one reason for this result, it was considered that NO_2^- acted as a source of nitroso function, a required function for NDMA formation in ozonation. On the other hand, NDMA concentration after DMPD ozonation in the absence of NO_2^- was 1600 ng L^{-1}, while that in the presence of NO_2^- was 3100 ng L^{-1}. As in the case of MB, NDMA concentration after DMPD ozonation increased by the presence of NO_2^-, but the degree of increase was lower. As one reason for this result, it was considered that the amino function of DMPD acted as a source of nitroso function. In the absence of NO_2^-, NDMA concentration after the ozonation of MB was lower than that of DMPD. However, in the presence of NO_2^-, NDMA concentration after the ozonation of MB was higher than that of DMPD. This might be due to the difference in the number of *N,N*-dimethylamino functions; two in MB and one in DMPD. That is, in the absence of coexisting compounds including NO_2^-, NDMA was formed as the result of ozonation of a compound with *N,N*-dimethylamino function and a source of a nitroso function. However, in the presence of NO_2^-, NO_2^- acted as a source of a nitroso function, and, therefore, the number of *N,N*-dimethylamino functions became the limiting factor for NDMA formation by ozonation.

NDMA concentrations after ozonation of MB and DMPD in the presence of TBA, a known HO· scavenger (Haag and Yao, 1992), were 180 and 3400 ng L^{-1}, respectively. Compared with that in the case of the absence of coexisting compounds, NDMA concentrations after ozonation decreased for MB and increased for DMPD. NDMA concentrations after the ozonation of target compounds are apparent values, that is, the difference between the NDMA formation and its decomposition during ozonation. For MB, it was considered that the NDMA formation associated with HO· was more significant than the NDMA decomposition by HO·, so that NDMA concentration after ozonation decreased by the presence of TBA. On the other hand, for DMPD, it was considered that the NDMA decomposition by HO· was more significant than the NDMA formation associated with HO·, so that NDMA concentration after ozonation increased by the presence of TBA. It is known that the reaction of HO· becomes significant at higher pH. As described above, NDMA concentration after MB ozonation increased with pH (Fig. 3). Thus, for MB, the effect of pH was consistent with that of the presence of TBA because the NDMA concentrations after ozonation became higher under the conditions of higher HO· concentration. However, for DMPD, the effect of pH was not consistent with that of the presence of TBA. One possible reason of the discrepancy of these two effects for DMPD was that the significance of the effects of HO· during ozonation (i.e., NDMA formation and its decomposition) might be dependent on pH even for the same NDMA precursor. The similar tendency was reported for the case of DMA (Andrzejewski et al., 2008). That is, it was reported that NDMA formation by DMA ozonation in the presence of TBA increased at pH 7.5 but decreased at pH 10.5.

NDMA concentrations after ozonation of MB and DMPD in the presence of H_2O_2 were 270 and 1700 ng L^{-1}, respectively. That is, NDMA concentrations after ozonation of both target compounds in the presence and absence of H_2O_2 were not markedly different. It was shown that NDMA formation by the ozonation of target compounds investigated is not affected by the presence of H_2O_2 when the pH was 7 and H_2O_2 concentration is 0.16 mM (5.3 mg L^{-1}), the concentration used in this study.

3.3. Effects of river water matrix

The effects of river water matrix on NDMA formation by ozonation of MB and DMPD were investigated. Initially, ozonation of river water samples without a target compound was conducted. NDMA concentrations before and after the ozonation of river water samples were 4.0 and 120 ng L^{-1} for Yodo river samples, respectively, and 4.7 and 18 ng L^{-1} for Tone river samples, respectively. It was shown that NDMA precursors in ozonation were present in both river water samples, particularly in those from the Yodo river (the reason for this is already described in Section 2***). Also, NDMA concentrations before the ozonation of river water samples with a target compound added were 5.1 ng L^{-1} for MB and 59 ng L^{-1} for DMPD in Yodo river samples, and 7.3 ng L^{-1} for MB and 36 ng L^{-1} for DMPD in Tone river samples. The reason of the NDMA detections by the addition of target compounds into the river waters was unclear. However, like the case of the presence of NO_2^-, there was a possibility that NDMA was formed by the reaction of the reagents of target compounds with some compounds in the river waters including NO_2^- (Table S1). These NDMA concentrations were much lower than those after ozonation with a target compound added, as described below.

Fig. 5 shows the effects of river water matrix on NDMA concentrations after the ozonation of MB and DMPD. NDMA concentrations after the ozonation of river water samples with a target compound added were 1100 ng L^{-1} for MB and 2800 ng L^{-1} for